

SUPPORTING INFORMATION

[Ru(Me₄phen)₂dppz]²⁺, a Light Switch for DNA Mismatches

Adam N. Boynton, Lionel Marcélis, and Jacqueline K. Barton

Division of Chemistry and Chemical Engineering, California Institute of Technology, Pasadena, California 91125, United States

Email: jkbarton@caltech.edu

Materials

All chemicals and starting materials were purchased from commercial vendors and used as received. Dipyrido[3,2-*a*:2',3'-*c*]phenazine (dppz) was prepared according to the literature.¹ UV-Visible spectra were recorded on a Beckman DU 7400 UV-Visible spectrophotometer (Beckman Coulter). Oligonucleotides were synthesized using standard phosphoramidite chemistry at Integrated DNA Technologies (Coralville, IA) and purified by HPLC using a C₁₈ reverse-phase column (Varian, Inc.) on a Hewlett-Packard 1100 HPLC. The copper complex Cu(phen)₂²⁺ was generated *in situ* by combining CuCl₂ with phen ligand in a 1:3 ratio.

Synthesis

Ru(Me₄phen)₂Cl₂: Following a modified literature report,² RuCl₃•*n*H₂O (0.217 g, 0.830 mmol), 3,4,7,8-Tetramethyl-1,10-phenanthroline (0.494 g, 2.09 mmol), and LiCl (0.298 g, 7.03 mmol) were combined in a Schlenk flask under argon. The contents were dissolved in anhydrous DMF (5 mL), and the solution was heated to 140°C and stirred for 4 h while being protected from light. The contents were cooled to room temperature, diluted with acetone (20 mL), and stored in the freezer overnight. The black precipitate was collected by vacuum filtration, washed three times with 5 mL portions of H₂O and three times with 5 mL portions of diethyl ether, and dried. The product was used subsequently without further purification (0.495 g, 73%).

Ru(Me₂bpy)₂Cl₂: RuCl₃•*n*H₂O (0.281 g, 1.07 mmol) was reacted with 5,5'-Dimethyl-2,2'-dipyridine (0.500 g, 2.71 mmol) and LiCl (0.385 g, 9.08 mmol) in DMF (15 mL) under the conditions described for the synthesis of Ru(Me₄phen)₂Cl₂. The product was isolated and used subsequently without further purification (0.304 g, 63%).

[Ru(Me₄phen)₂dppz]X₂ (X = PF₆ or Cl): Dppz ligand (0.025 g, 0.089 mmol) was combined with Ru(Me₄phen)₂Cl₂ (0.057 g, 0.089 mmol) in ethylene glycol (8 mL) and heated to 130°C and stirred for 5 h. The reaction was cooled to room temperature and diluted with H₂O (8 mL). Excess NH₄PF₆ was added to precipitate the product, which was collected by filtration, washed copiously with H₂O and diethyl ether, and dried. (0.084 g, 82%). ESI(+)-MS (*m/z*): [M/2]⁺ found 428.2. The complex was converted to its water-soluble Cl salt by anion exchange chromatography (Sephadex QAE) and further purified by preparative HPLC using an isocratic method of 65% MeOH and 35% H₂O (containing 0.1% TFA) over 60 min. ¹H NMR (500 MHz, DMSO-*d*₆) δ 9.58 (dd, *J* = 8.2, 1.3 Hz, 2H), 8.54 (dd, *J* = 6.3, 3.4 Hz, 2H), 8.52 (d, *J* = 0.9 Hz, 4H), 8.22 (dd, *J* = 6.6, 3.4 Hz, 2H), 8.13 (dd, *J* = 5.4, 1.3 Hz, 2H), 7.90 (m, 4H), 7.76 (s, 2H), 2.82 (d, *J* = 1.3 Hz, 12H), 2.27 (d, *J* = 3.7 Hz, 12H). The complex was again converted to its Cl salt by anion exchange chromatography to remove TFA anions present from the HPLC purification.

[Ru(Me₂bpy)₂dppz]X₂ (X = PF₆ or Cl): Dppz ligand (0.240 g, 0.851 mmol) was combined with Ru(Me₂bpy)₂Cl₂ (0.304 g, 0.563 mmol) in ethylene glycol and reacted as described for the Me₄phen complex, and the product was collected as its PF₆ salt (0.521 g, 88.8%). ESI(+)-MS (*m/z*): [M/2]⁺ found 376.2. The complex was converted to its water-soluble Cl salt by anion exchange chromatography (Sephadex QAE) and further purified by preparative HPLC using a gradient of H₂O (with 0.1% TFA) to CH₃CN over 60 min. ¹H NMR (500 MHz, DMSO-*d*₆) δ 9.62 (dd, *J* = 8.2, 1.3 Hz, 2H), 8.71 (d, *J* = 8.4 Hz, 2H), 8.67 (d, *J* = 8.4 Hz, 2H), 8.52 (m, 2H), 8.21 (m, 4H), 8.04 (m, 4H), 7.94 (dd, *J* = 8.4, 1.9 Hz, 2H), 7.54 (dt, *J* = 1.8, 0.8 Hz, 2H), 7.48 (dt, *J* = 1.4, 0.7 Hz, 2H), 2.26 (d, *J* = 0.7 Hz, 6H), 2.08 (d, *J* = 0.7 Hz, 6H). The

complex was again converted to its Cl salt by anion exchange chromatography to remove TFA anions present from the HPLC purification.

Steady-State Luminescence Measurements

Luminescence spectra were recorded on an ISS-K2 spectrofluorometer at 25°C. The Ru complex was excited at 440 nm, and emission spectra were integrated from 564-820 nm. The Cl salt of the complex was used for all experiments. In all cases, [DNA] is defined as the concentration of full sequence.

Titrations of $[\text{Ru}(\text{Me}_4\text{phen})_2\text{dppz}]^{2+}$ with the well-matched and mismatched duplexes (Figure S1) were used to determine the binding affinity of the complex for well-matched and mismatched sites. For the titration with well-matched DNA, the binding affinity is evaluated using the McGhee-Von Hippel method;³ a value of $6.75 \cdot 10^4 \text{ M}^{-1}$ per base pair is obtained with an occupational factor, n , of 2.3.

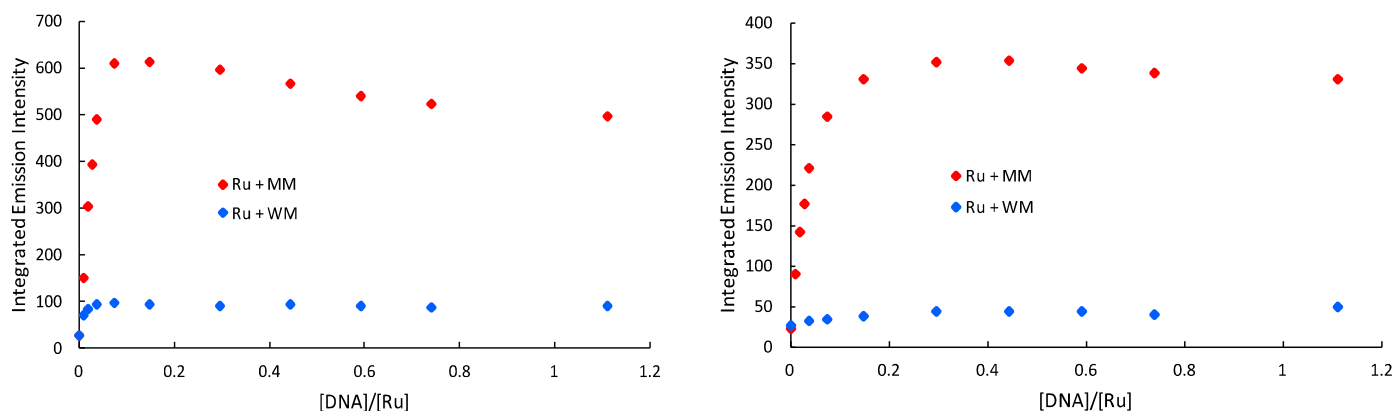
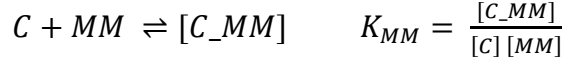


Figure S1: Steady-state luminescence titrations of $[\text{Ru}(\text{Me}_4\text{phen})_2\text{dppz}]^{2+}$ with well-matched (blue) and mismatched (red) DNA. *Left plot:* samples prepared in 5 mM tris, 50 mM NaCl, pH 7.5. *Right plot:* samples prepared in 5 mM tris, 200 mM NaCl, pH 7.5. $[\text{Ru}] = 2 \mu\text{M}$, $\lambda_{\text{ex}} = 440 \text{ nm}$. Emission spectra were integrated from 564-820 nm.

In order to evaluate the binding affinity of the complex for the mismatched site, we first must consider two competing equilibria, expressed below.





K_{ass} describes the binding equilibrium between the complex, C , and the well-matched base pair sites, BP , in the DNA. K_{MM} describes the binding equilibrium between the complex and the mismatched site, MM .

Next, we will express the total concentration of complex as C_c ; this is kept constant throughout the titration. We can then define the various molar fractions for the complex as follows:

$$f = \frac{[C]}{C_c}, \text{ the molar fraction of free complex.}$$

$$b = \frac{[C_BP]}{C_c}, \text{ the molar fraction of complex bound to WM base pairs.}$$

$$m = \frac{[C_MM]}{C_c}, \text{ the molar fraction of complex bound to MM sites.}$$

Additionally, we express the total concentration of duplex as C_{ODN} ; this value increased throughout the titration. The variable R is introduced as being equal to the ratio C_{ODN}/C_c , and in our titration the luminescence of the complex is measured as a function of this ratio R . The luminescence intensity, I , can be expressed as a function of R as follows:

$$I = \alpha b + \beta m$$

where α and β are equal to the relative emissivity of complex associated with BP and MM , respectively.

We must define two final parameters: x , the the ratio of well-matched sites to mismatched sites in the duplex, and p , the occupational factor which takes into account the possible inhibition of binding by two complexes in close vicinity. We are now ready to express the equilibrium

concentrations of free BP and MM sites as follows:

$$[BP] = n (1 - x) C_{ODN} - p [C_{BP}] = n (1 - x) C_{ODN} - p b C_M$$

$$[MM] = n x C_{ODN} - [C_{MM}] = n x C_{ODN} - m C_M$$

Thus,

$$\frac{[BP]}{C_C} = n (1 - x) R - p b \text{ and } \frac{[MM]}{C_C} = n x R - m$$

The binding equilibrium equations are thus rewritten as:

$$K_{ass} = \frac{b}{f C_C (n (1-x) R - p b)} \text{ and } K_{MM} = \frac{m}{f C_C (n x R - m)}$$

The expression of b and m as functions of f can thus be obtained:

$$K_{ass} f C_C (n (1 - x) R - p b) - b = 0$$

$$b = \frac{K_{ass} C_C n (1 - x) R f}{1 + K_{ass} C_C p f}$$

$$K_{MM} f C_C (n x R - m) - m = 0$$

$$m = \frac{K_{MM} C_C n x R f}{1 + K_{ass} C_C f}$$

With

$$1 = f + b + m$$

$$0 = f - 1 + \frac{K_{ass} C_C n (1 - x) R f}{1 + K_{ass} C_C p f} + \frac{K_{MM} C_C n x R f}{1 + K_{ass} C_C f}$$

$$0 = (f - 1)(1 + K_{ass} C_C p f)(1 + K_{ass} C_C f) + K_{ass} C_C n (1 - x) R f (1 + K_{ass} C_C f) \\ + K_{MM} C_C n x R f (1 + K_{ass} C_C p f)$$

The expression of the intensity of luminescence, I , can be written as follows:

$$I = \alpha \frac{K_{ass} C_C n (1 - x) R f}{1 + K_{ass} C_C p f} + \beta \frac{K_{MM} C_C n x R f}{1 + K_{ass} C_C f}$$

The fitting process is realized by an iterative solving to the expression of f using the previous equation.

A global fitting on the data obtained from the well-matched and mismatched titrations is performed (occupational factor set to 2) and yield the values of $K_{ass} = 6.8 \cdot 10^4 \text{ M}^{-1}$ per base pair and $K_{MM} = 1.8 \cdot 10^6 \text{ M}^{-1}$ per mismatched site for the 200 mM NaCl condition and $K_{ass} = 1.1 \cdot 10^5 \text{ M}^{-1}$ per base pair and $K_{MM} = 9.7 \cdot 10^6 \text{ M}^{-1}$ per mismatched site for the 50 mM NaCl condition. The errors are evaluated to be equal to 10 %.

When comparing titrations in 50mM and 200mM NaCl, we observe two changes. First for both duplexes, the emission intensities at saturating values for 200mM NaCl are approximately half those obtained at 50 mM NaCl, consistent with the increase in ionic strength leading to a decrease in emission intensities observed previously. Second we find that the ionic strength affects the shape of the binding curve. At 50 mM NaCl we see a maximum emission intensity upon titration followed by a decrease in emission as DNA/Ru increases; at 200 mM NaCl this effect is less dramatic. We attribute this difference to less non-specific DNA association at higher ionic strength.

Time-Resolved Luminescence Measurements

Time-resolved spectroscopic measurements were carried out at the Beckman Institute Laser Resource Center, and were conducted using instrumentation that has been described.⁴ Briefly, a 460 nm light produced by OPO pumped with a 10 Hz, Qswitched Nd:YAG laser (Spectra-Physics Quanta-Ray PRO-Series) was used as an excitation source (pump pulse duration ≈ 8 ns). The emitted light was detected at 660 nm with a photomultiplier tube (Hamamatsu R928) following wavelength selection by a double monochromator (Instruments SA DH-10). Scattered laser light was removed from the detectors using suitable filters. The samples were held in 1 cm path length quartz cuvettes (Starna) equipped with stir bars and irradiated at 460 nm with 500–1000 laser pulses at 3 mJ/pulse. Kinetic traces were fit to exponential equations of the form $I(t) = a_0 + \sum a_n \exp(-t/\tau_n)$, where $I(t)$ is the signal intensity as a function of time, a_0 is the intensity at long time, a_n is a pre-exponential factor that represents the relative contribution from the n th component to the trace, and τ_n is the lifetime of the n th component, convoluted with a Gaussian function to take into account the Instrument Response Function (fwhm = 8ns). The errors are evaluated to be equal to 5%, but the uncertainty on the short component (associated with complexes bound to well-matched DNA, *i.e.* 33-35 ns) being close to the IRF time characteristic is subject to a greater error (+/- 8 ns).

Models of $[\text{Ru}(\text{Me}_4\text{phen})_2\text{dppz}]^{2+}$ Binding to Well-matched and Mismatched DNA

The binding constants obtained for the complex with the mismatched and well-matched sites indicate that the complex preferentially binds to mismatched DNA. The relative emissivity determined during the fitting process, *i.e.* 40 for complexes associated with well-matched sites and 380 for complexes associated with mismatched sites, also correlates with the differential

luminescence lifetimes. As such, ruthenium bound to the mismatched site should be more protected from quenching than complex bound *via* intercalation at well-matched sites. To gain more insight regarding the local environment around the DNA-bound complex, we used published crystal structures^{5,6} of DNA to model the binding of $[\text{Ru}(\text{Me}_4\text{phen})_2\text{dppz}]^{2+}$. In one model, we inserted Δ - $[\text{Ru}(\text{Me}_4\text{phen})_2\text{dppz}]^{2+}$ into an AC mismatch *via* the minor groove (Figure 4 of main text and Figure S2), and oriented the complex in such a way as to maximize the protective environment around the dppz ligand while avoiding steric clashes with the DNA. As seen in Figures 4 and S2, the dppz ligand is capable of being deeply inserted into the mismatch site, allowing greater protection from quenching. In the other model, we intercalated the complex at a well-matched site from the major groove, again minimizing steric clashes between the Me_4phen ligands and the DNA. In this model, we oriented the complex in both a head-on fashion (Figure S2) and a side-on orientation (Figure 4). In the head-on orientation, both phenazine nitrogen atoms are relatively well-surrounded by the duplex, but in the side-on approach, we see that dppz is more exposed to quenching.

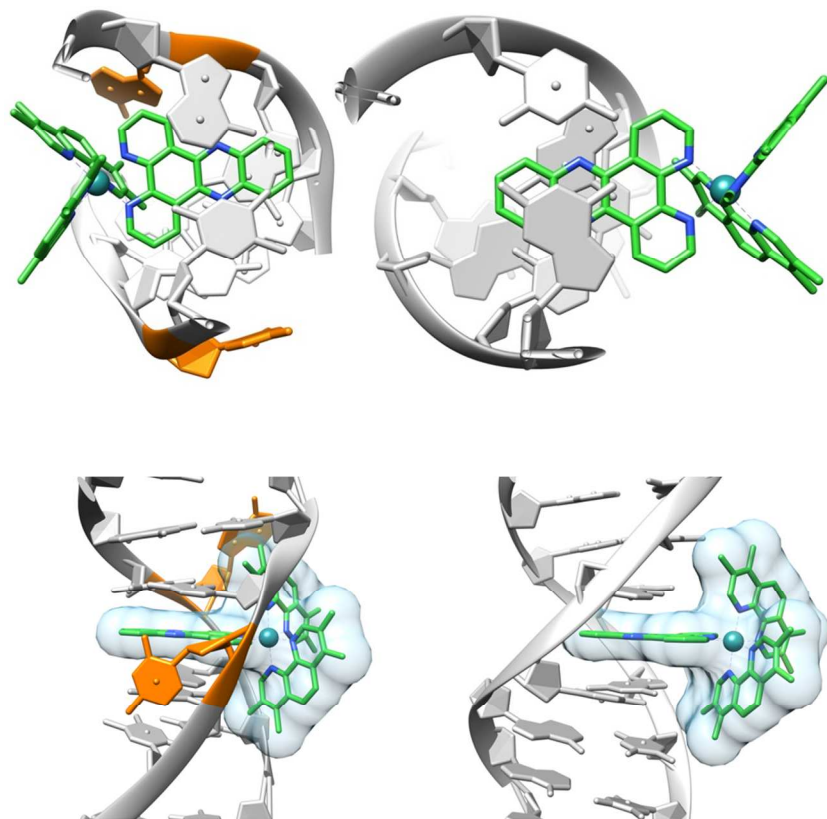


Figure S2: *Top:* Axial views, down the helical axis, of Δ -[Ru(Me₄phen)₂dppz]²⁺ modeled into the crystal structures of DNA duplexes. *Top left:* Metalloinsertion at the mismatch site from the minor groove; the extruded mismatch bases are shown in orange. *Top right:* Head-on intercalation at a well-matched site from the major groove. *Bottom:* Side-views of (*left*) metalloinsertion at the mismatch from the minor groove and (*right*) head-on intercalation at a well-matched site from the major groove. The optimization and visualization were carried out using UCSF Chimera program.

MTT Cytotoxicity Assay

This assay was performed as described previously.⁷ HCT116N and HCT116O cells were plated in 96-well plates (50,000 cells/well), treated with the Ru concentrations indicated in Figure 3 of the main text, and incubated for 72 hours (37°C, 5% CO₂, humidified atmosphere). After this incubation period, MTT was added to the cells (Roche Cell Proliferation Kit I) and the cells were incubated for an additional 4 hours. Insoluble formazan crystals were dissolved in solubilizing reagent (Roche) over 24 hours (37°C, 5% CO₂, humidified atmosphere). The solubilized formazan was quantified at 570 nm with 690 nm as the reference wavelength. Percent cell viability was calculated as a function of formazan formed in the Ru-treated cells relative to untreated cells.

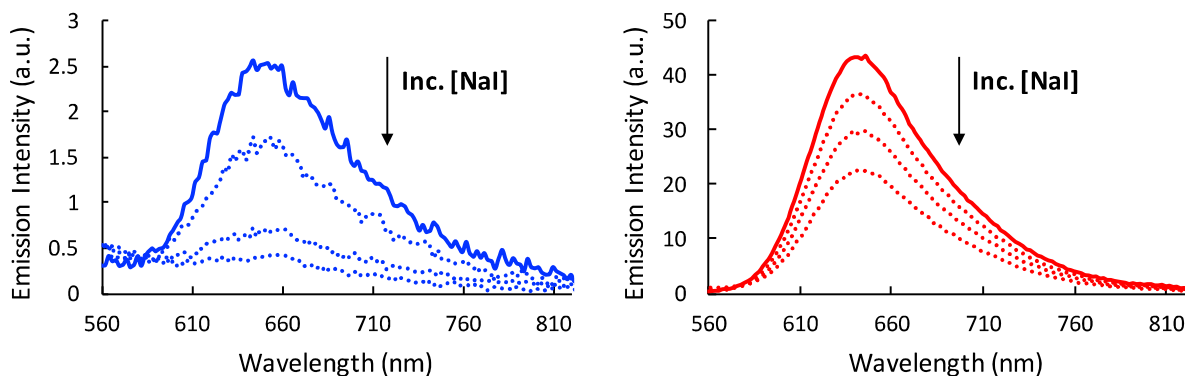


Figure S3: Steady-state NaI quenching of [Ru(Me₄phen)₂dppz]²⁺ (2 μM) bound to well-matched (left, blue) and mismatched (right, red) DNA (2 μM). Solid lines indicate no NaI present, and dotted lines represent increasing NaI concentrations of 25, 50, and 75 mM, respectively. $\lambda_{\text{ex}} = 440$ nm. Samples prepared in 5 mM tris, 200 mM NaCl, pH 7.5. The DNA sequences are as in Figure 1 of the main text.

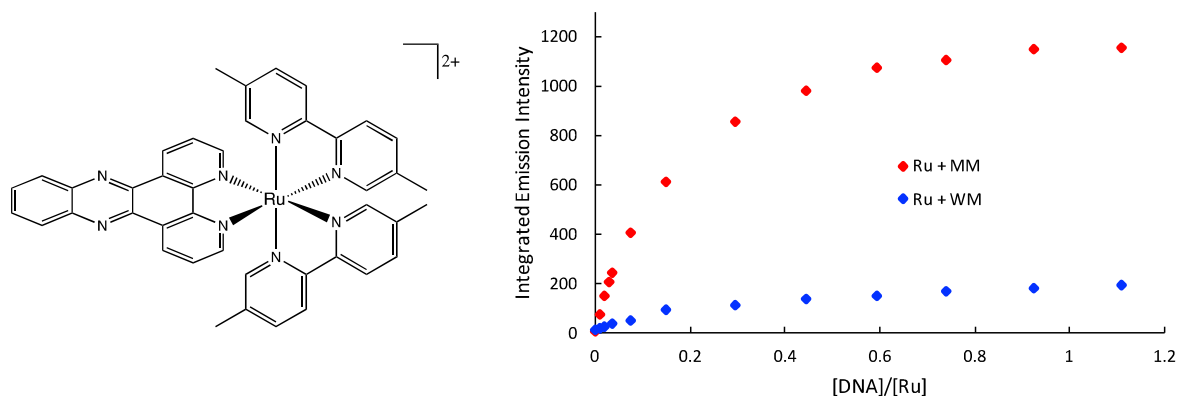


Figure S4: (Left) Schematic of $[\text{Ru}(\text{Me}_2\text{bpy})_2\text{dppz}]^{2+}$. (Right) Steady-state luminescence titrations of $[\text{Ru}(\text{Me}_2\text{bpy})_2\text{dppz}]^{2+}$ with well-matched (blue) and mismatched (red) DNA. Samples prepared in 5 mM tris, 200 mM NaCl, pH 7.5. $[\text{Ru}] = 2 \mu\text{M}$, $\lambda_{\text{ex}} = 440 \text{ nm}$. Emission spectra were integrated from 550-850 nm.

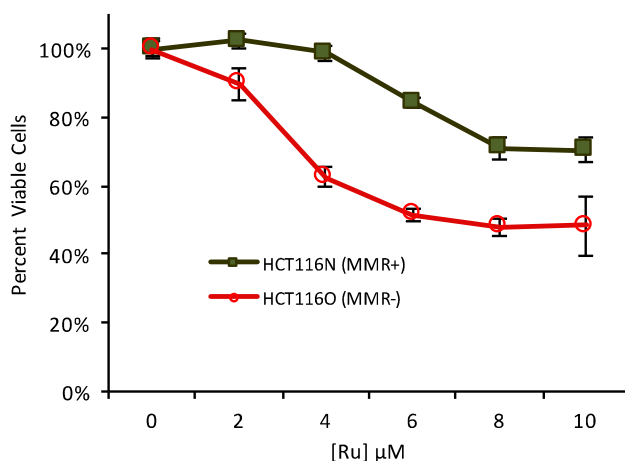


Figure S5: Differential cytotoxicity of $[\text{Ru}(\text{Me}_4\text{phen})_2\text{dppz}]^{2+}$ towards HCT116N and HCT116O cell lines. Cells were plated in a 96-well format (5×10^4 cells/well) and treated with the indicated Ru concentrations for 72 h. Following this incubation period, the cells were labeled with MTT for 4 h. Metabolically active cells reduce the MTT to produce its insoluble formazan, which is then solubilized and quantified by its absorbance at 570 nm. The percent viability is the ratio of formazan absorbance in cells treated with ruthenium to the absorbance in untreated cells.

Supporting References

1. Dickerson, J.E.; Summers, L.A. *Aust. J. Chem.* **1970**, *23*, 1023-1027.
2. Nakabayashi, Y.; Watanabe, Y.; Nakao, T.; Yamauchi, O. *Inorg. Chim. Acta* **2004**, *357*, 2553-2560.
3. McGhee, J.D.; von Hippel, P.H. *J. Mol. Biol.* **1974**, *86*, 469 - 489.
4. Dempsey, J. L.; Winkler, J. R.; Gray, H. B. *J. Am. Chem. Soc.* **2010**, *132*, 1060–1065.
5. Pierre, V.C.; Kaiser, J.T.; Barton, J.K. *Proc. Natl. Acad. Sci.* **2007**, *104*, 429-434.
6. Kielkopf, C.L.; Erkkila, K.E.; Hudson, B.A.; Barton, J.K.; Rees, D.C. *Nat. Struct. Biol.* **2000**, *7*, 117-121.
7. Mosmann, T.J. *J. Immunol. Methods* **1983**, *65*, 55-63.